Elastic Anisotropy of Earth's Inner Core

Anatoly B. Belonoshko,[1,2]* Natalia V. Skorodumova,[3] Anders Rosengren,[2,4] Börje Johansson[1,3,5]

Earth's solid-iron inner core is elastically anisotropic. Sound waves propagate faster along Earth's spin axis than in the equatorial plane. This anisotropy has previously been explained by a preferred orientation of the iron alloy hexagonal crystals. However, hexagonal iron becomes increasingly isotropic on increasing temperature at pressures of the inner core and is therefore unlikely to cause the anisotropy. An alternative explanation, supported by diamond anvil cell experiments, is that iron adopts a body-centered cubic form in the inner core. We show, by molecular dynamics simulations, that the body-centered cubic iron phase is extremely anisotropic to sound waves despite its high symmetry. Direct simulations of seismic wave propagation reveal an anisotropy of 12%, a value adequate to explain the anisotropy of the inner core.

Science **319**, 797 (2008);
DOI: 10.1126/science.1150302

Elastic Anisotropy of IC

- Morelli & Dziewonski [1986]
  - Travel Time Residual of the PKIKP

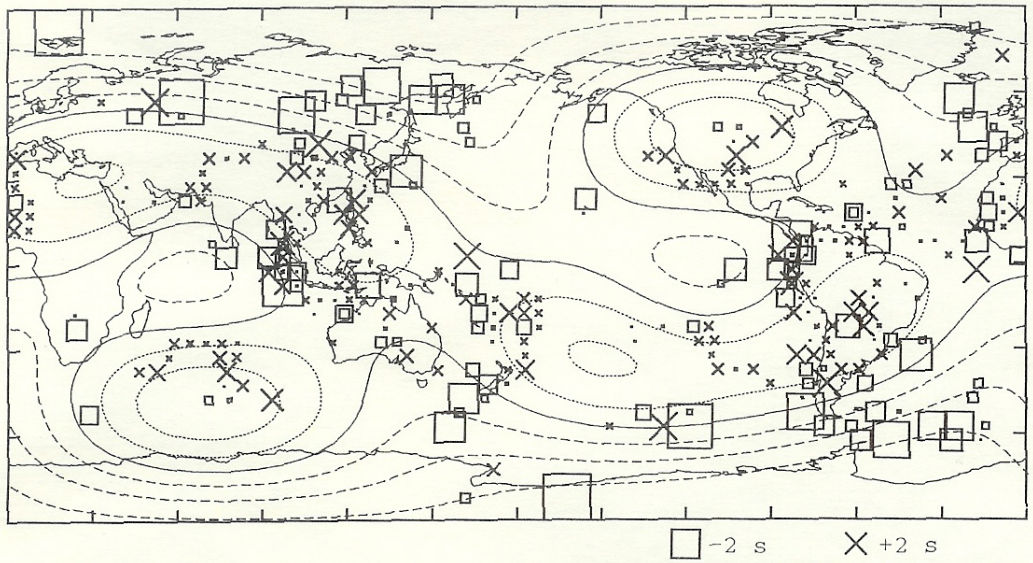

Fig. 1. Travel-time anomalies for nearly vertical rays (170° – 180°) after correction for station anomalies and lower mantle and CMB structures. Each symbol is the average in a bin of a subdivision of 1654 equi-areal cells. Each residual is plotted both at the source and receiver locations. The spherical harmonic expansion truncated at degree 4 is shown by the contour lines; contour interval is 0.4 s.

Elastic Anisotropy of IC

- By introducing anisotropy with cylindrical symmetry aligned with the earth's rotation axis, data with different epicentrical distance become consistent
  - $v_p = v_{eq} \times (1 + \varepsilon \cos^2\zeta + \sigma \cos^2\zeta \sin^2\zeta)$
    - $\varepsilon = 0.032(5)$
    - $\sigma = -0.064(15)$

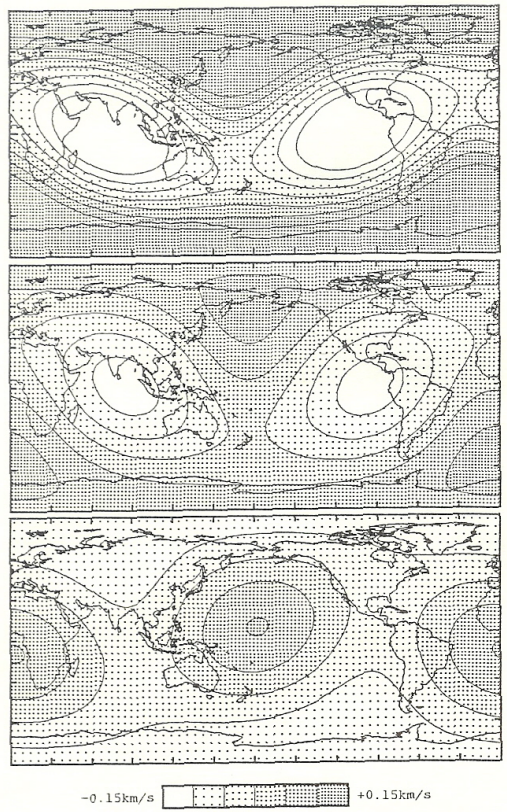

Fig. 2. Models for lateral heterogeneity at the top of the inner core. These patterns decrease in amplitude with depth as r^2. Only degree 2 of the expansion is shown. Top – model obtained using data from subset R5; middle – model from set R4; bottom – model from set R2. The scale is ± 0.15 km/s for all the plots to facilitate the comparison. Note that values in the top panel are by far out of scale: anomalies exceed 0.5 km/s.

Epicentrical Distance

170-180°

155-170°

120-135°

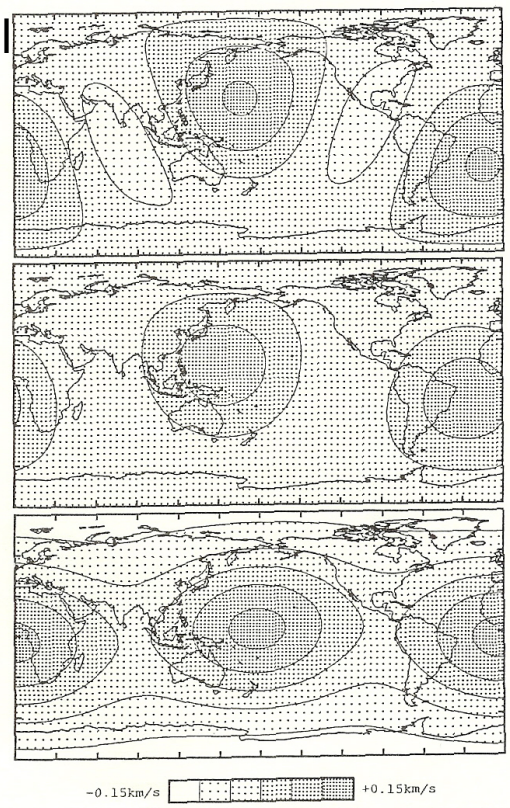

Fig. 4. Same as Figure 2, but corrected for anisotropy in the inner core. The three models, derived from the three independent datasets R5, R4 and R2, are now highly correlated.

Morelli & Dziewonski [1986]

Successive studies for anisotropy of IC

- Creager (1992)
  - Differential travel time of PKP (BC) and PKIKP (DF)
  - Axisymmeteric anisotropy in the outer most portions of the inner core
  - 3~4 % faster in the direction of the spin axis

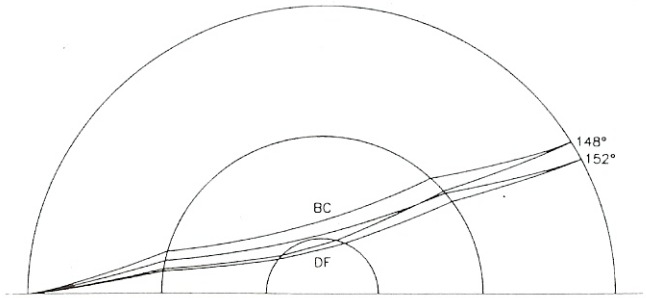

FIG. 1 Ray paths of P'_{DF} entering the solid inner core and P'_{BC} turning in the liquid outer core from a surface-focus earthquake to stations at epicentral distances of 148° and 152°.

More complicated anisotropy

- Song and Helmberger [1995]
  - Comparison of PKIKP and PKiPK
  - The top 150 km of IC is weakly anisotropic and the top 60 km is no anisotropic
- Souriau and Romanowicz [1997]
  - Comparison of PKP(DF) and PKP(BC)
  - Faster velocity, stronger attenuation
- Ishii & Dziewonski [2002]
  - Comparison of PKP(DF) with PKP(AB) or PKP(BC)
  - Strong anisotropy in the innermost inner core (IMIC) with a 300 km radius.
  - The slowest direction of wave propagation in ~45° from the equatorial plane
- Beghein & Trampert [2003]
  - Free oscillation (normal mode) of the Earth
  - P-wave anisotropy sign changed around radius of 400 km
    - Faster in the axis direction in shallower depth
  - S-wave anisotropy is strong in the lower part
    - Faster in the axis direction
- Cao & Romanowicz [2007]
  - Examine Ishii & Dziwonski [2002] and Beghein & Trampert [2003]
  - Ishii & Dziwonski [2002] is better but,
  - IMIC radius of 500 km, the slowest direction is between 50 to 55°.

Current explanation of IC anisotropy

- Preferred orientation of hcp iron
  - HCP iron is considered to be stable under the IC conditions
  - HCP iron should have anisotropy because it has a hexagonal symmetry

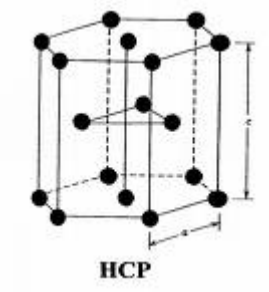

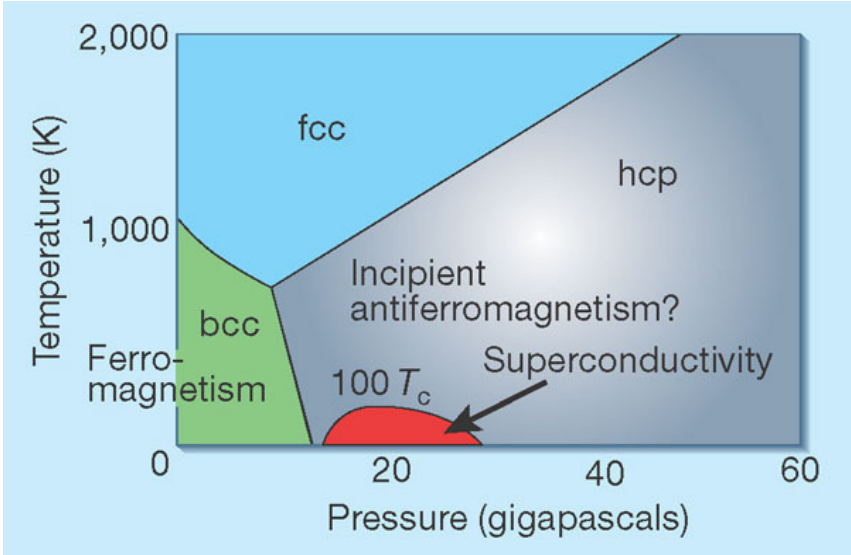

Anisotropy of hcp iron

- Stixrude & Cohen [1995]
  - Ab initio calculation of elasticity of fcc & hcp irons
    - 0 K & HP, ρ = 13 g/cm^3
  - V_p is fastest in the [001] direction in hcp iron
    - However, anisotropy of hcp iron is much smaller than fcc iron
  - [001] of Hcp iron should nearly perfectly aligned in the spin direction of the Earth

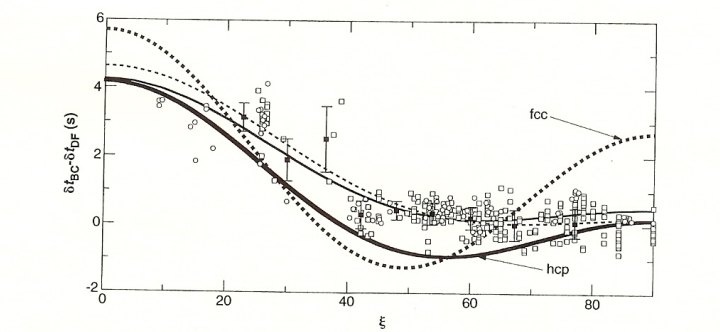

Fig. 2. Plot of BC − DF travel time anomalies as a function of the angle ξ between the inner core ray segment and Earth's spin axis for Δ = 150° (see text). The forward models described in the text for an inner core consisting of an hcp aggregate (bold solid line) and a cylindrically averaged fcc aggregate (bold dashed line) are compared with observations and the best fits to the two data sets [circles and thin solid line (*7*), squares and thin dashed line (*3*)]. The binned data of (*3*) are also shown (solid squares with error bars).

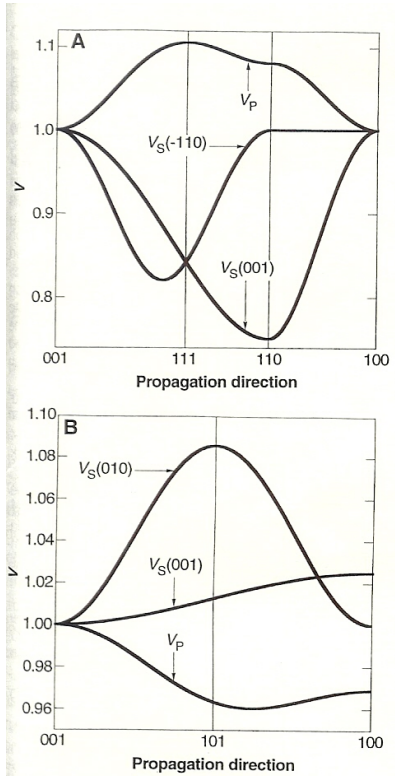

fcc

hcp

Fig. 1. Single-crystal velocities in fcc (**A**) and hcp (**B**) iron at a density of ρ = 13 Mg/m^3. Planes of polarization are indicated for *S* waves. Velocities are normalized to those corresponding to propagation along [001], for which shear-wave velocities are degenerate in both crystals. For fcc, velocities along [001] (in kilometers per second) are 11.28 (V_P) and 6.98 (V_S); for hcp, 12.13 (V_P) and 11.84 (V_S).

Decrease in anisotropy of hcp iron

- If c/a is ideal (1.633), no anisotropy
  - the distances with 12 nearest neighbors are the same.
- With increasing temperature, c/a approaches to 1.633
- Small anisotropy should be present under the inner core conditions

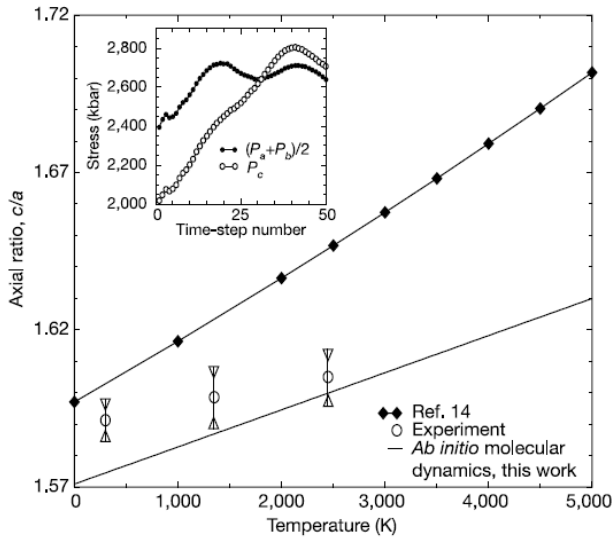

Figure 3 The axial ratio of h.c.p. iron as a function of temperature. The ratio is calculated at a constant volume (7.2 Å^3 per atom) using *ab initio* molecular dynamics[12] and compared with experimental[15,26] (taken at pressures above 1.5 Mbar, triangles indicate error bars) and calculated previously[14] (interpolated) data. The insertion demonstrates the time dependence of stresses in the basal plane and along the *c* axis at $T = 5{,}000$ K, $V = 7.2$ Å^3 per atom and $c/a = 1.65$. It is clear that during the first 50 time-steps, while thermal equilibrium is not yet reached, P_c (stress along the *c* axis) becomes larger than P_a, providing the incorrect impression that the *c*/*a* ratio must be increased to obtain equal stresses. The neglect of thermal equilibrium led to a very high calculated *c*/*a* ratio[14], where all atoms in a computational cell were frozen except one. In our method all atoms are allowed to move, which seems to lead to much better agreement with experiment, particularly when the temperature increases. Our data are approximated by a straight line for clarity. At 5,000 K the ratio is close to ideal ($c/a = 1.633$).

Belonoshoko et al. [2003]

Possibility of bcc iron

- Brown & McQueen [1986]
  - Observed ε -"γ"-Liq phase transitions in the shock Hugoniot
- Ross et al. [1990]
  - B&M: too high pressure for "γ" phase
  - Introduce BCC phase (α')

Brown & McQueen [1986]

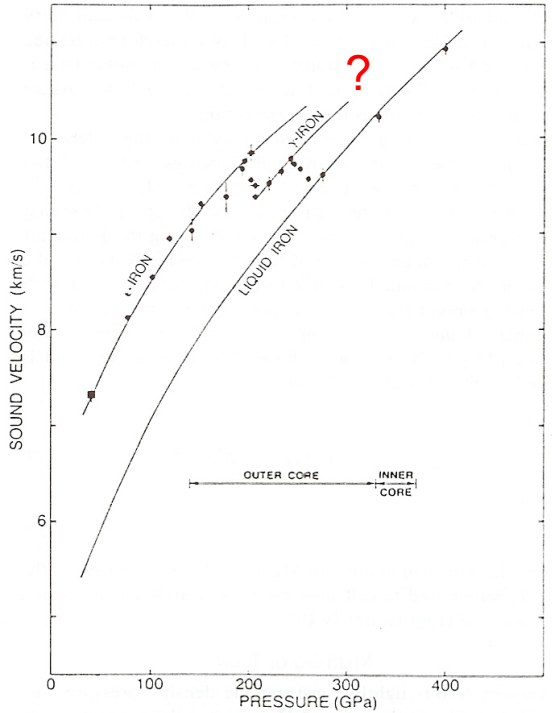

Fig. 3. Rarefaction velocities for iron on the Hugoniot as a function of pressure. Circles are present data. The square is from *Barker and Hollenbach* [1974].

Ross et al. [1990]

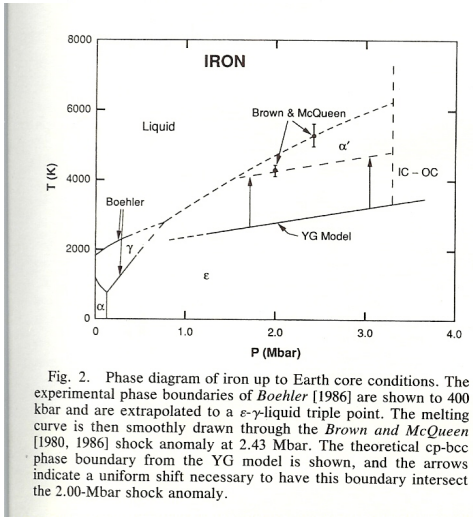

Fig. 2. Phase diagram of iron up to Earth core conditions. The experimental phase boundaries of *Boehler* [1986] are shown to 400 kbar and are extrapolated to a ε-γ-liquid triple point. The melting curve is then smoothly drawn through the *Brown and McQueen* [1980, 1986] shock anomaly at 2.43 Mbar. The theoretical cp-bcc phase boundary from the YG model is shown, and the arrows indicate a uniform shift necessary to have this boundary intersect the 2.00-Mbar shock anomaly.

Stabilization of BCC phase

- Stabilized by high entropy at high temperatures
  - Belonoshko et al. [2003]
    - Molecular dynamics based on EAM
    - Above 120 GPa, bcc iron appears at high temperatures
  - Vocadlo et al. [2003]
    - Ab initio molecular dynamic calculation
    - BCC iron is getting more stable, but HCP is more stable for pure iron
    - For stability of BCC, impurity is necessary
- Experimentally reported recently
  - Dubrovinsky et al. [2007]

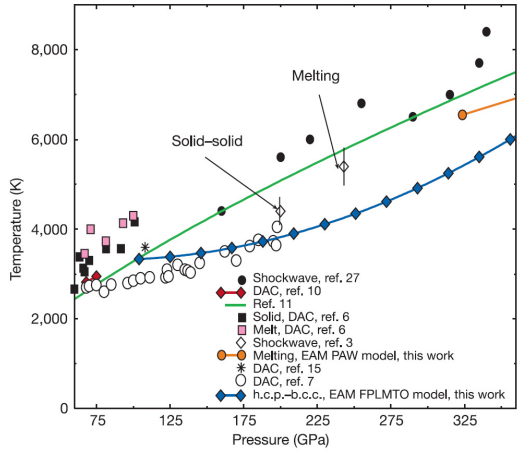

Belonoshoko et al. [2003]

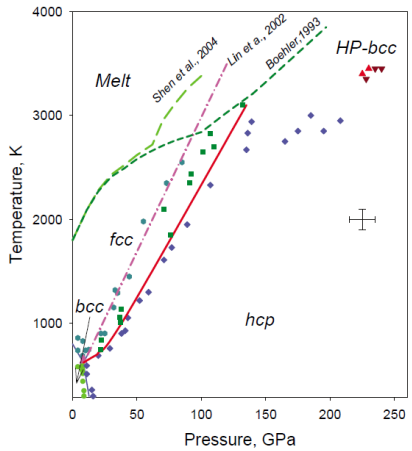

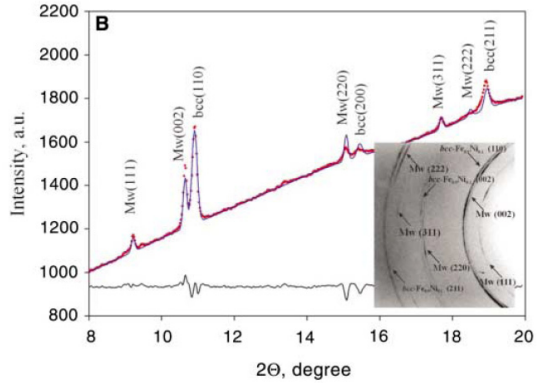

Dubrovinsky et al. 2007

This study

- Simulation of sound wave propagation
- Molecular dynamics simulation
- The embedded-atom method (EAM)

Embedded atom method (EAM)

- An approximation of potential for metal
- Combination of short-range repulsion and many body attraction terms
- $E_{tot} = \Sigma_i F_i(\rho_i(R_i)) + 1/2 \Sigma_{i,j} \phi(r_{i,j})$
  - ϕ: short-range electrostatic pair potential
    - $\phi(r_{i,j}) = \varepsilon\ (a/r_{i,j})^n$,
  - ρ_i: electron density of the host without atom *i*
  - Simplification: the electron density is given by a linear superposition of the electron densities of the constituent atoms:
    - $\rho_i(R_i) = \Sigma_{i,j} \rho(r_{i,j})$
    - $\rho(r_{i,j}) = (a/r_{i,j})^m$,
  - $F(\rho_i(R_i)) = -\varepsilon\ C \rho_i(R_i)^{1/2}$

Samples

- BCC Single crystal 1
  - Orientating [100] in Z direction
  - 2 atoms in a unit cell
- BCC Single crystal 2
  - Orientating [111] in Z, [110] in X, [112] in Y
  - 12 atoms in a unit cell
- Polycrystalline
  - 2,000,000 atoms heated to 10,000 K for melting
  - 4 bcc crystals whose [001] is aligned in Z axis and rotated around Z axis
  - Cooled to 6800 K and 3.6 Mbar
  - The sample size is 240Å
- HCP iron

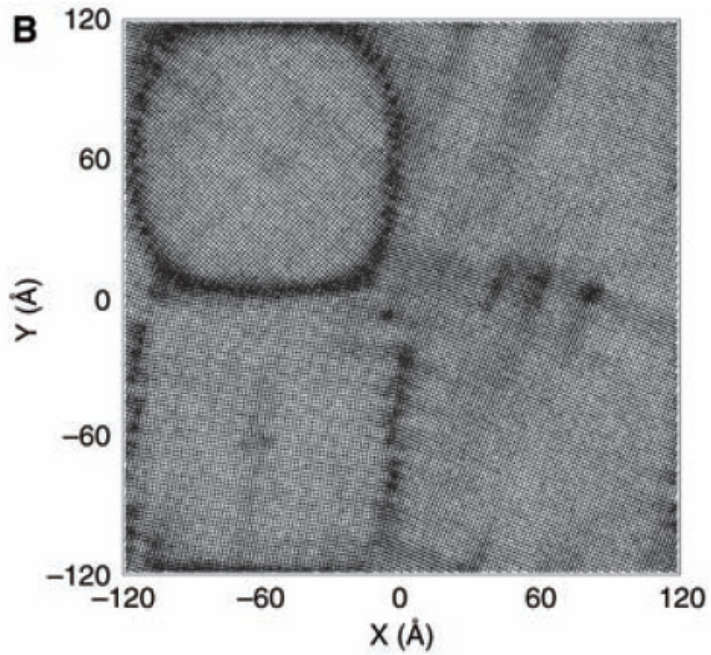

Simulation of sound wave propagation

- Shifting the two halves of the samples toward each other by 0.3Å along the X axis
- Energy pulse is concentrated in 15 % of interatomic distance
- Simulation keeping N (number of particles), E (total energy) and V (volume)
- Propagation of the energy pulse
  - $A^x_i = (1/N_i^{atoms}) \Sigma_{atom\ in\ i th\ layer}\ f^x_{atom}$
  - Calculate energy in each layer normal to the X axis
- Wave is noticed not by the displacement of atom but by the force
  - Force in EAM is 8 power of distance
  - Force is much easier to detect than displacement

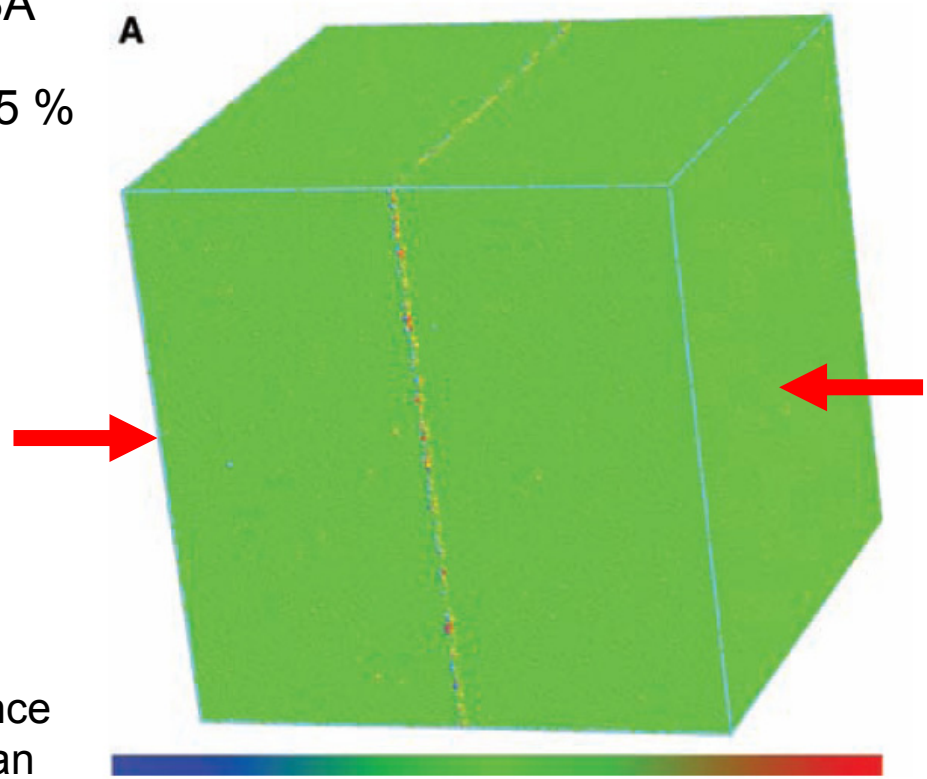

Propagation of sound waves

time

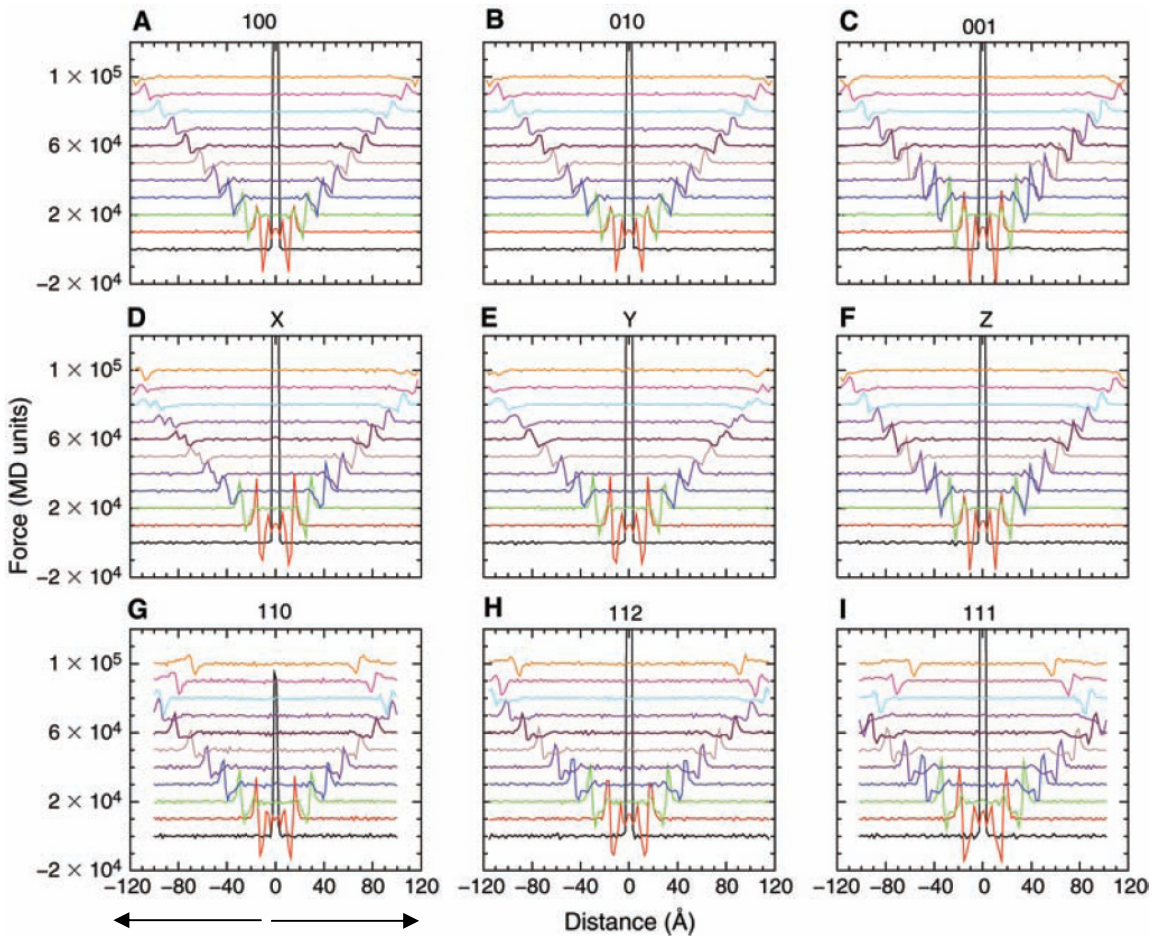

Single crystal 1

Polycrystal

Single crystal 2

Results

Table 1. Calculated velocities of sound waves under *PT* conditions of inner core.

	Sample*	*P* (GPa)	*T* (K)	Direction†	Velocity (km/s)	
1	bcc, single	361.0	6589	100	12.05	
2	bcc, single	360.3	6587	010	12.02	
3	bcc, single	360.2	6595	001	12.16	
4	bcc, poly	366.7	6918	*X*	12.86	
5	bcc, poly	364.8	6929	*Y*	12.60	
6	bcc, poly	364.3	6850	*Z*	12.02	[001] aligned
7	bcc, single	364.8	6644	110	13.06	
8	bcc, single	362.7	6640	112	12.90	
9	bcc, single	364.6	6924	111	13.60	
10	hcp, single	368.5	6860	001	13.89	
11	hcp, single	369.1	7002	100	13.89	
12	hcp, single	364.5	6726	110	13.57	

*The sample description provides crystal structure (hcp or bcc) and whether the crystal is single or polycrystal. †The direction of the initiated sound wave is given by providing crystallographic direction *hkl*, where *hkl* are the integer vector components. For example, 111 in the bcc crystal means direction of the big diagonal in the cubic unit cell, and 001 means direction along the edge of the cell.

- Precision of velocity : 0.1 km
  - Compare 1, 2 and 3: 12.05, 12.02 and 12.16 km
- <001> :slowest, <111>: fastest, difference 1.5(1) km
- Defect has no impact on the velocity
  - Compare 1,2 and 3 with 6

Essential isotropy of hcp iron

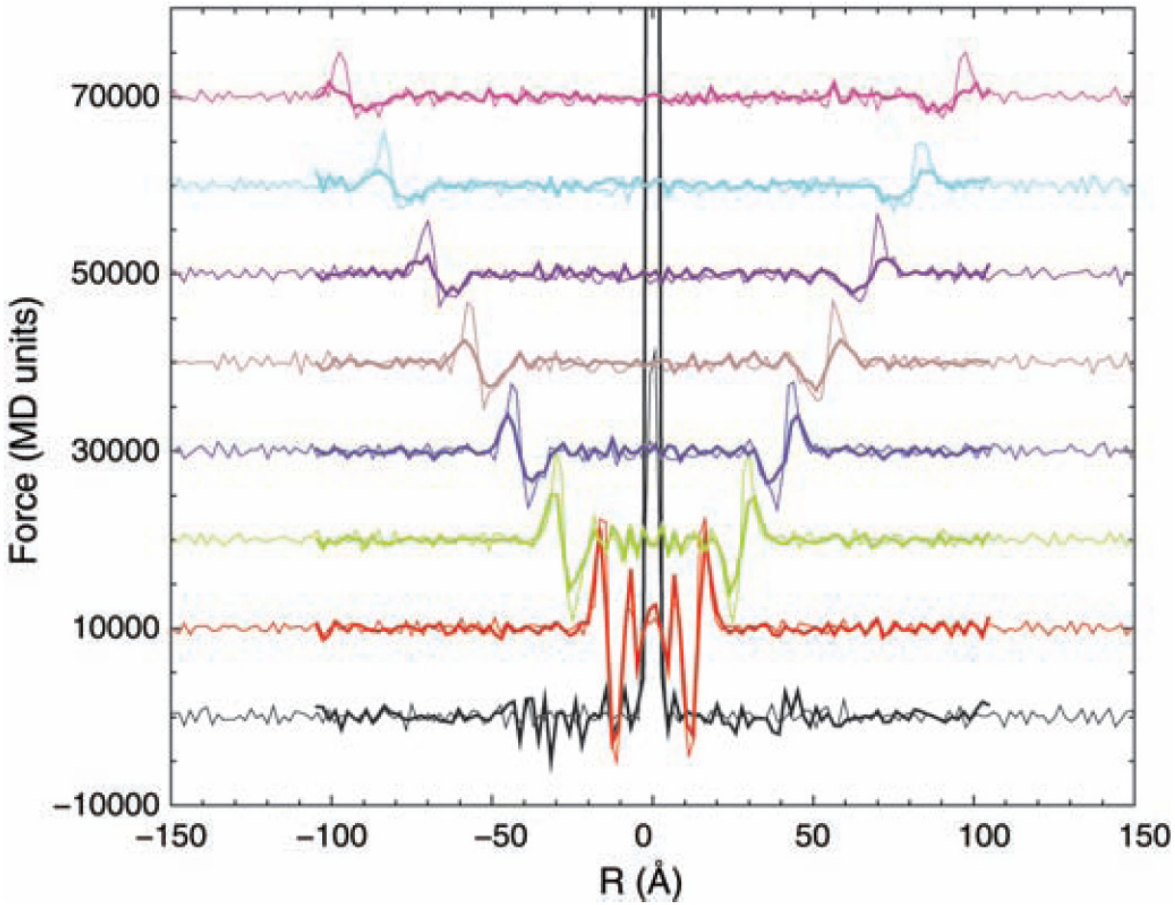

Thin line [001]
Thick line [100]

Waves of the thin and thick lines are in the same positions

Why hcp is isotropic?

- The 12 first neighbors in the ideal hcp structure are located in the same distance
- The structure is identical in the 12 directions

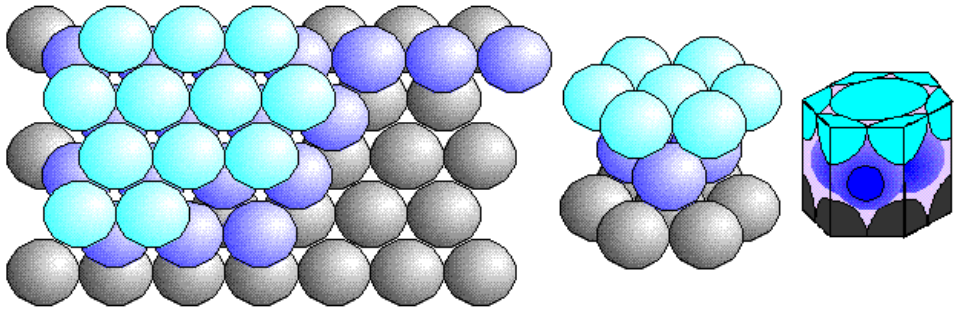

ABAB Layer Stacking

Hexagonal Structure

Why bcc is anisotropic?

- The 8 first neighbors (<111> directions) whose distance is slightly shorter than in hcp structure
- The 6 second neighbors (<100> directions) are located in the distance larger than the nearest neighbors in the hcp structure
- Largely different between <100> and <111> directions

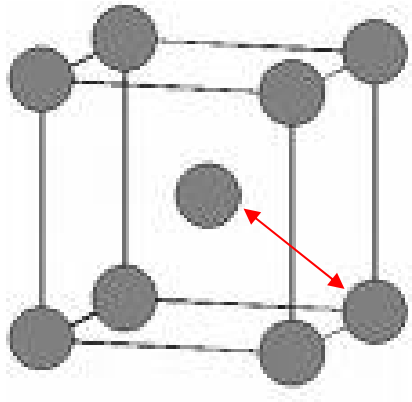

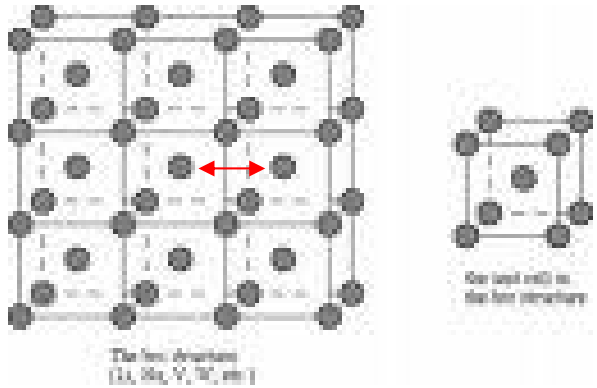

Explanation of IC anisotropy

- Bcc crystals with [111] aligned with the Earth's spin axis
- Only 30 %
  - Difference between [111] and [100] is 15 %
  - IC anisotropy: 3~4 %
- Velocity of bcc is closer to IC than hcp
  - IC: 11.26 km/s, bcc: 12.0-12.9 km/s, hcp: 13.6-13.9 km/s.

IC is mixture of bcc and hcp?

- Different seismic observations give different results
  - Ishii & Dziewonski [2002]
    - Strong anisotropy in the innermost inner core (IMIC) with a 300 km radius.
  - Beghein & Trampert [2003]
    - P-wave anisotropy sign changed around radius of 400 km
      - Faster in the axis direction in shallower depth
- Such difference may reflect the mixture of hcp and bcc irons?